# Supporting Information

## Encapsulation of BiOCl nanoparticles in N-doped carbon nanotubes as highly efficient anode for potassium ion batteries

Qianqian Yang,[a,#] Hao Li,[b,#] Chuanqi Feng,[a,#] Quanwei Ma,[b,#] Longhai Zhang,[b,*] Rui Wang,[b] Jianwen Liu,[a,*] Shilin Zhang,[c] Tengfei Zhou,[b] Zaiping Guo,[c] Chaofeng Zhang[b,*]

[a]*Collaborative Innovation Center for Advanced Organic Chemical Materials Co-constructed by the Province and Ministry, Ministry of Educational Key Laboratory for the Synthesis and Application of Organic Functional Molecules, College of Chemistry and Chemical Engineering, Hubei University, Wuhan 430062, China*

[b]*Institutes of Physical Science and Information Technology, Engineering Laboratory of High Performance Waterborne Polymer Materials of Anhui Province, Leibniz Research Center for Materials Science, Anhui Graphene Engineering Laboratory, Key Laboratory of Structure and Functional Regulation of Hybrid Material (Ministry of Education), Anhui University, Hefei 230601, China*

[c]*School of Chemical Engineering and Advanced Materials, The University of Adelaide, Adelaide, South Australia, Australia*

[#] These authors contributed equally to this work

Corresponding Authors: zlhedu@163.com (L. Zhang); jianwen@hubu.edu.cn (J. Liu); cfz@ahu.edu.cn (C. Zhang)

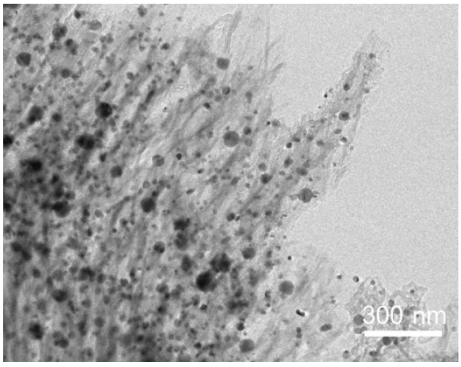


**Fig. S1.** TEM image of Co@N-CNTs.

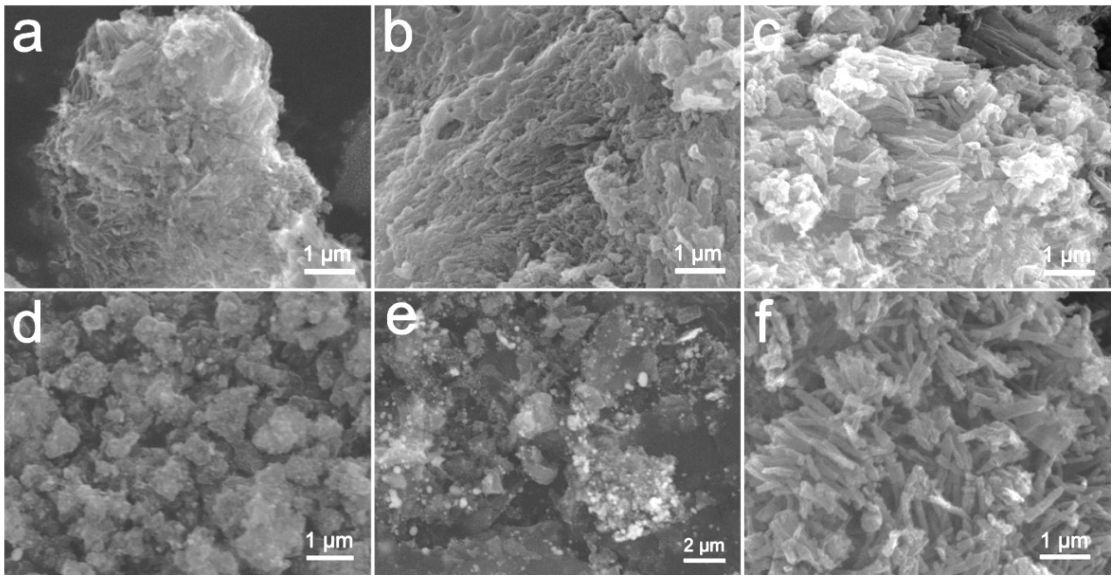


**Fig. S2.** SEM images of (a) Co@N-CNTs-750, (b) Co@N-CNTs-800, (c) Co@N-CNTs-850, (d) Co@NC, (e) Co@BC, and (f) N-CNTs, respectively.

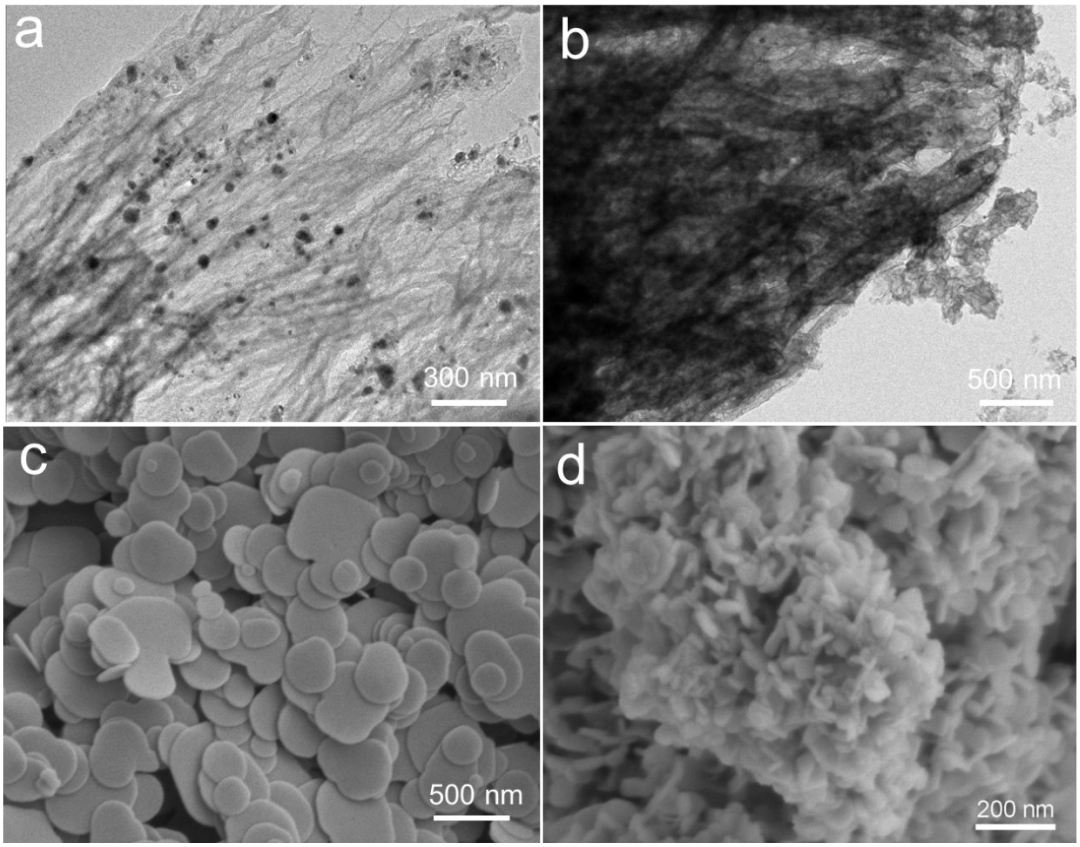


**Fig. S3.** TEM images of (a) BiOCl@N-CNTs-1 and (b) BiOCl@N-CNTs-2. SEM images of (c) BiOCl, and (d) BiOCl@C.

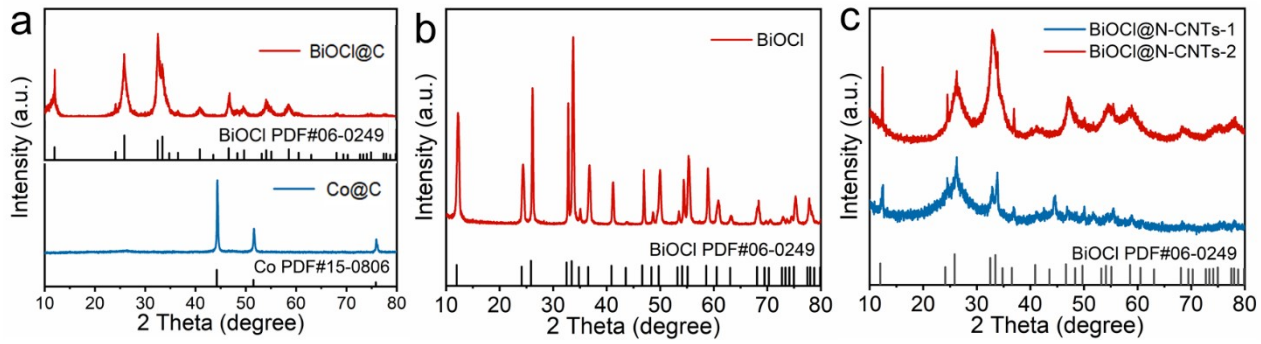


**Fig. S4.** XRD patterns of synthesized (a) Co@C and BiOCl@C, (b) BiOCl, and (c) BiOCl@N-CNTs-1 and BiOCl@N-CNTs-2.

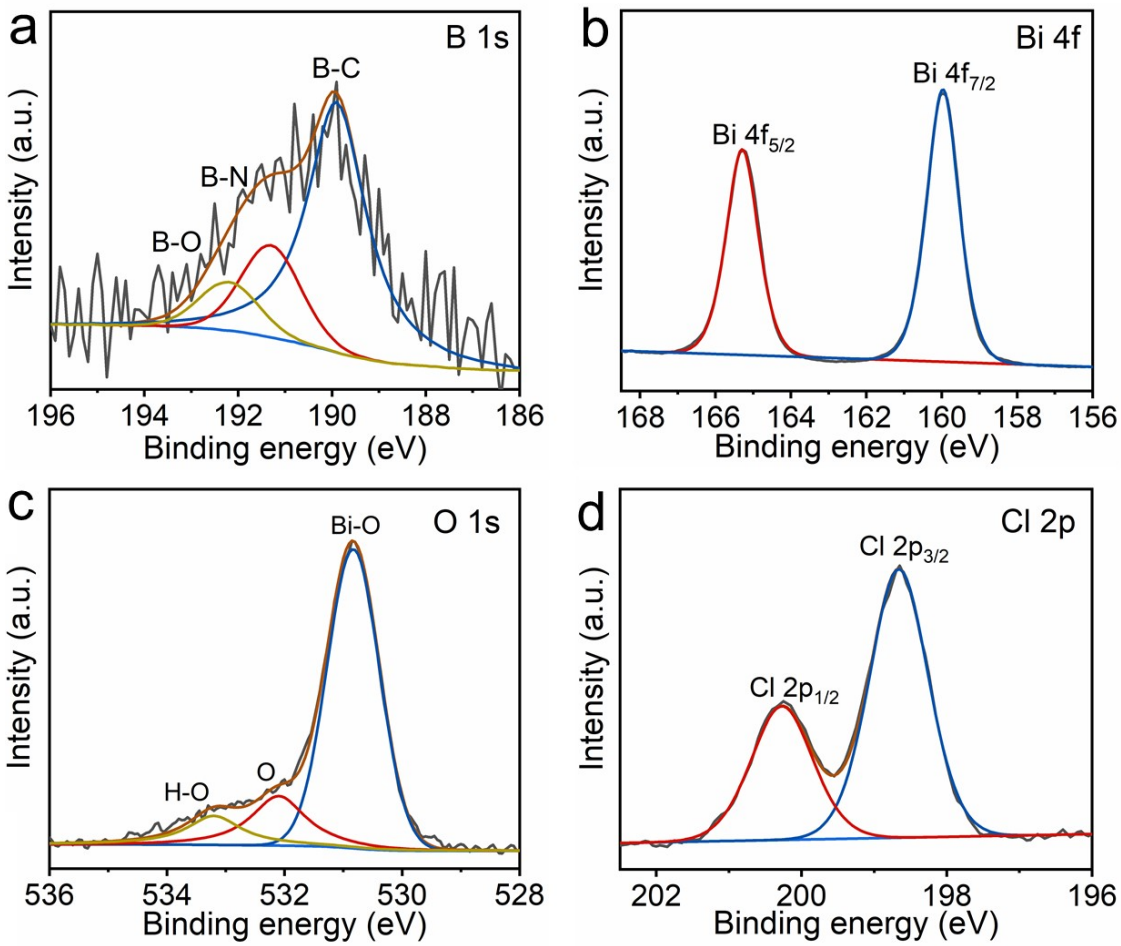


**Fig. S5.** (a) High-resolution XPS spectra of B 1s for BiOCl@N-CNTs, and (b) Bi 4f, (c) O 1s, and (d) Cl 2p for BiOCl@C.

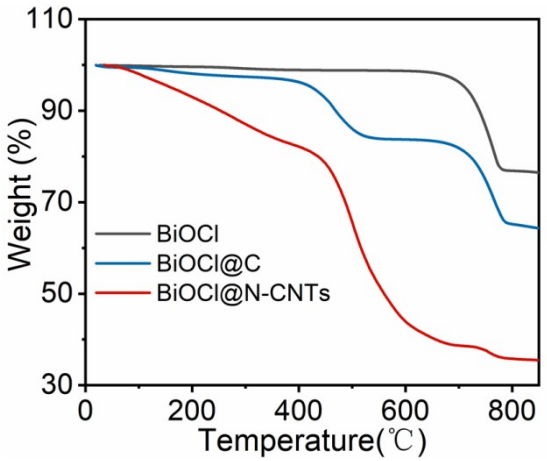


**Fig. S6.** TG curves of BiOCl, BiOCl@C and BiOCl@N-CNTs.

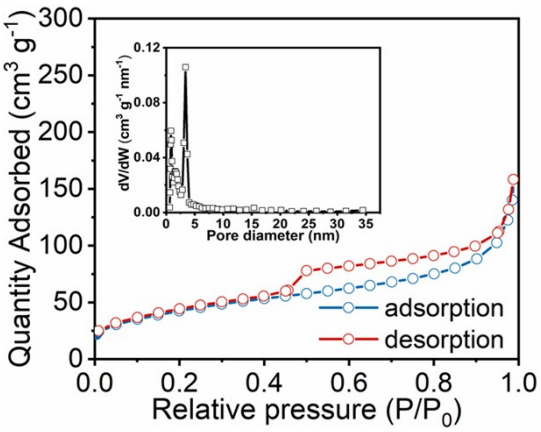


**Fig. S7.** Nitrogen adsorption-desorption isotherm of BiOCl@C (the inset shows the pore size distributions).

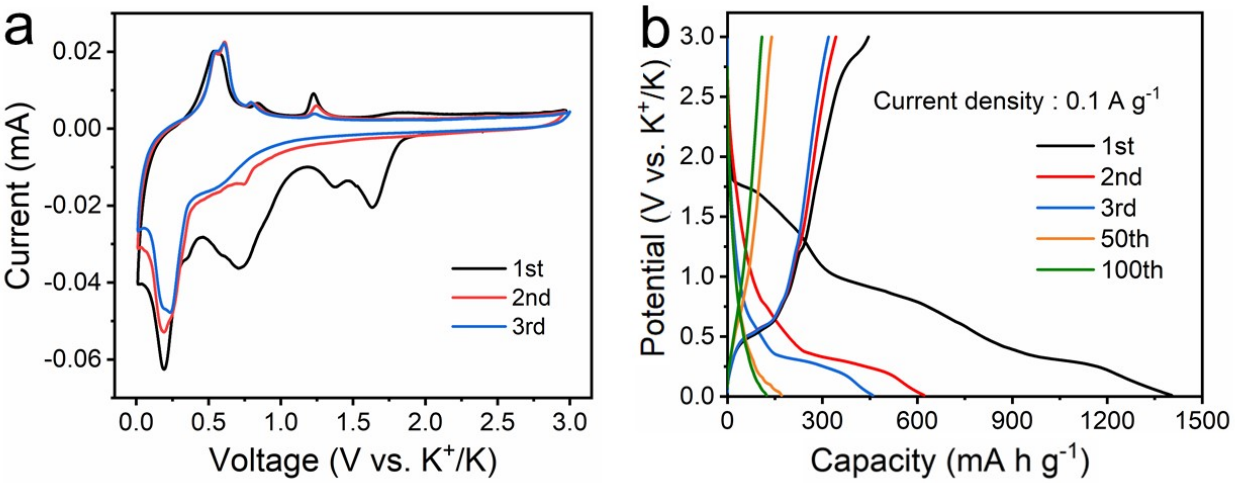


**Fig. S8.** (a) CV curves of the BiOCl@C at a scan rate of 0.1 mV $s^{-1}$ within a voltage range of 0.01−3.0 V. (b) Discharge and charge profiles of the BiOCl@C at 0.1 A $g^{-1}$.

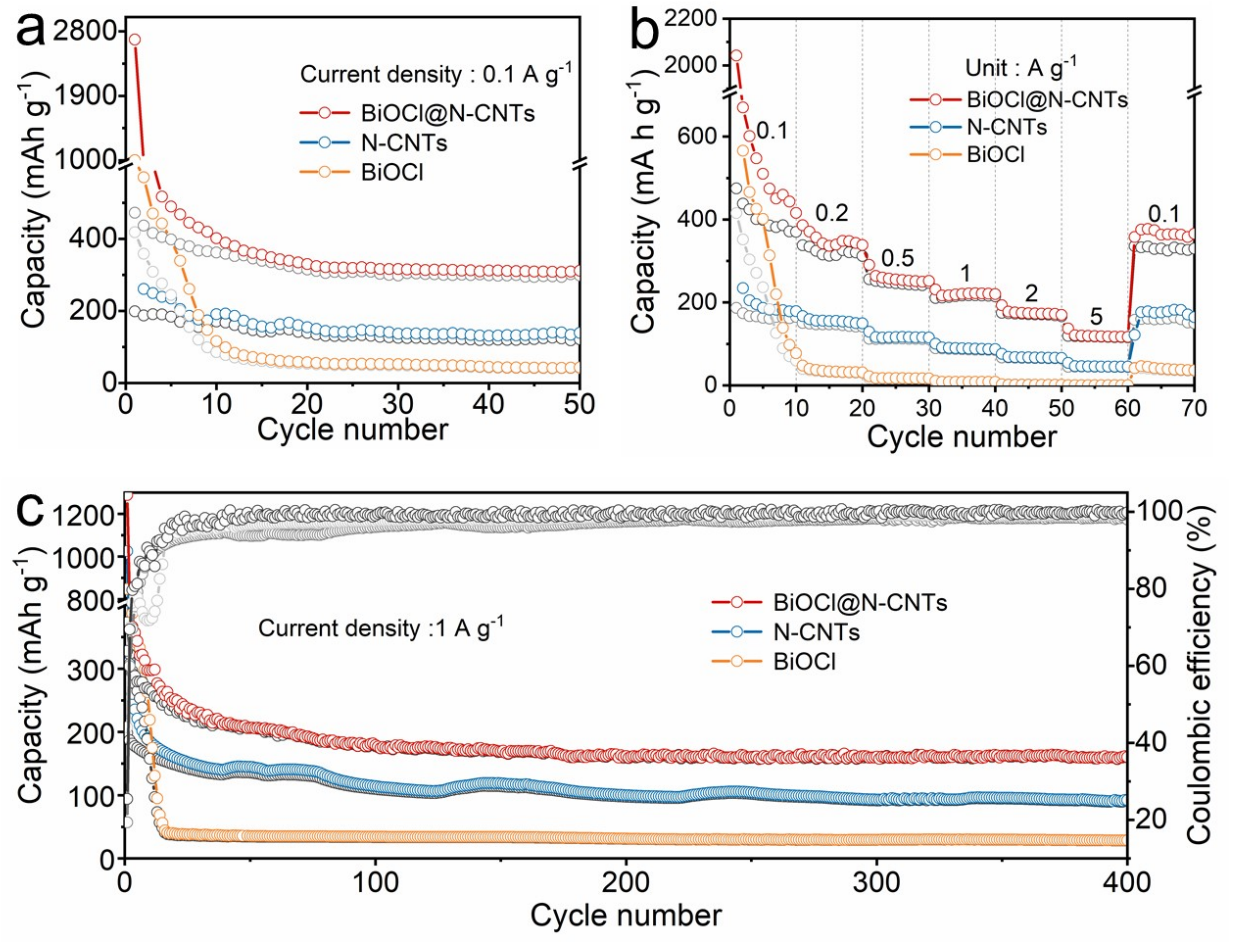


**Fig. S9.** (a) Cycling performance at 0.1 A $g^{-1}$, (b) Rate capability, and (c) Long-term cycling performance at 1.0 A $g^{-1}$ of BiOCl@N-CNTs, BiOCl and N-CNTs.

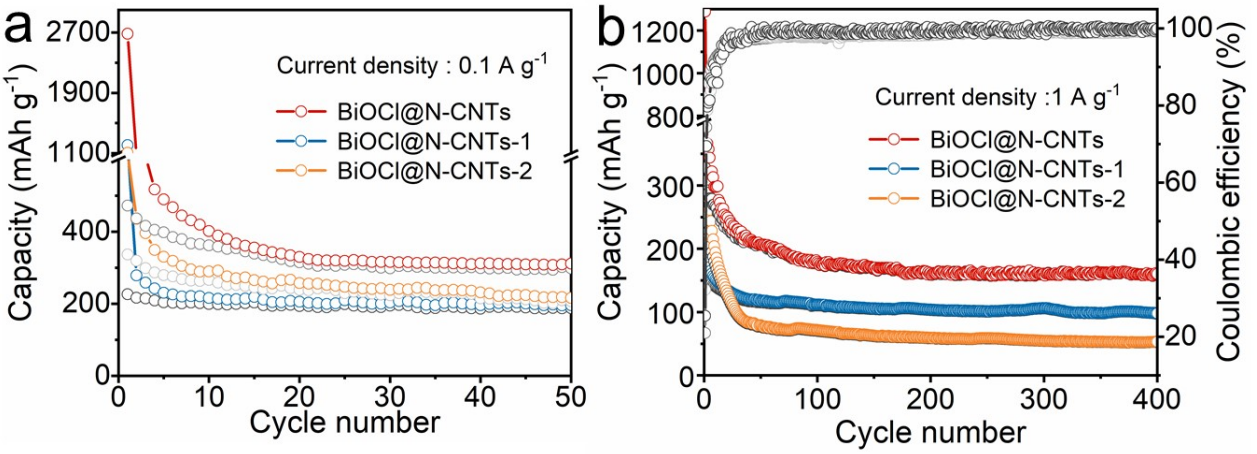


**Fig. S10.** (a) Cycling performance at 0.1 A $g^{-1}$, and (b) Long-term cycling performance at 1.0 A $g^{-1}$ of BiOCl@N-CNTs, BiOCl@N-CNTs-1 and BiOCl@N-CNTs-2.

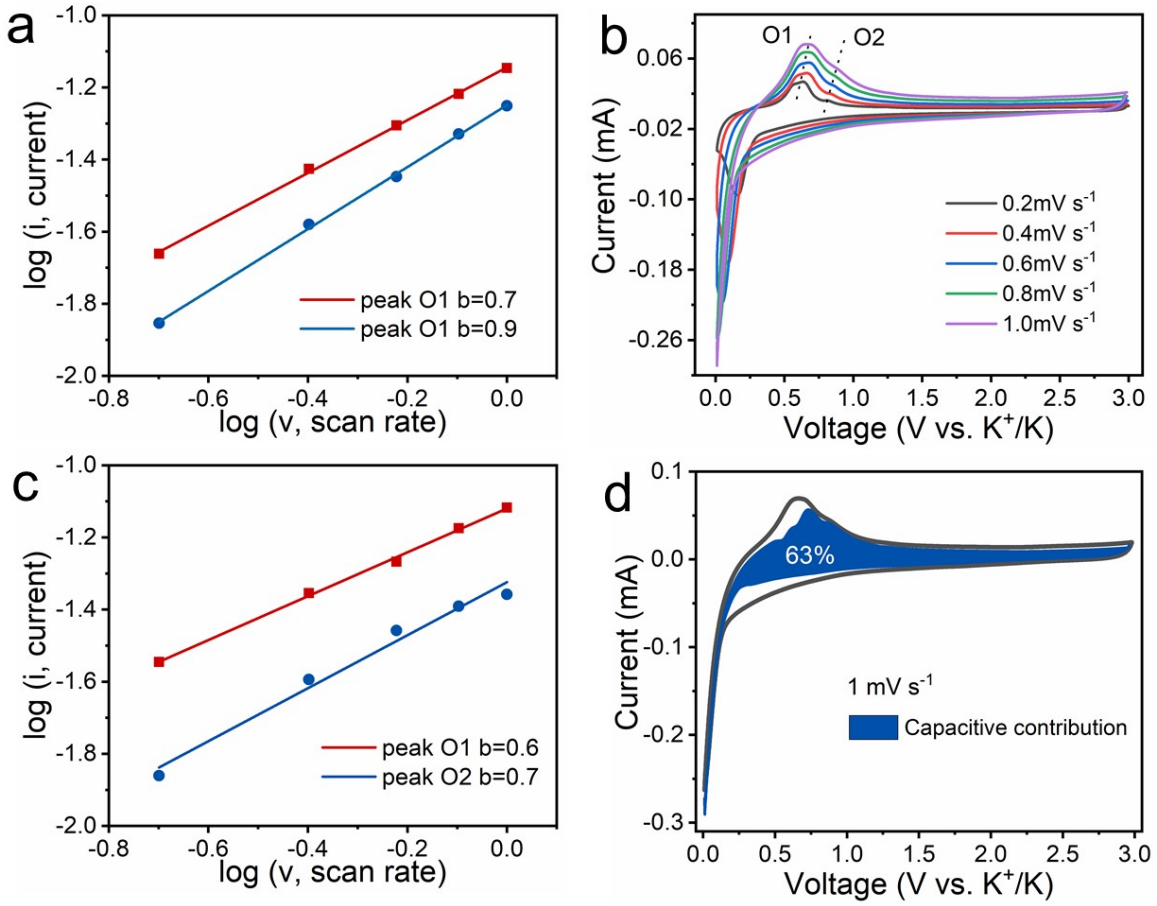


**Fig. S11.** (a) The relationship of log i and log v of BiOCl@N-CNTs. (b) CV curves of the BiOCl@C at different scan rates, and (c) corresponding relationship of log i and log v. (d) Capacitive contribution in total CV curve of BiOCl@C.

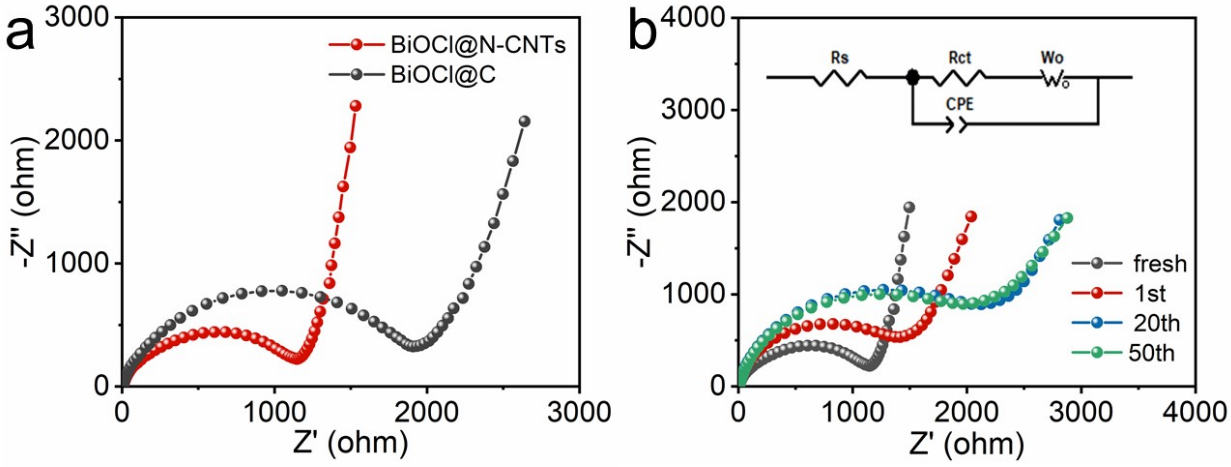


**Fig. S12.** (a) EIS of BiOCl@N-CNTs and BiOCl@C before cycle. (b) EIS of BiOCl@N-CNTs in different cycles.

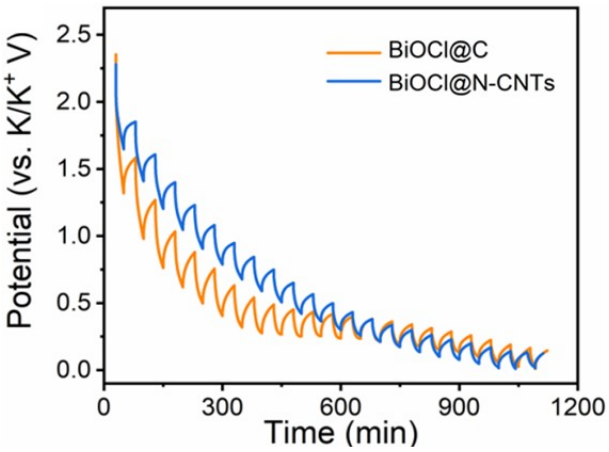


**Fig. S13.** GITT profiles of the BiOCl@C and BiOCl@N-CNTs during the discharge process after 20 cycles.

**Table S1.** The capacity and high-rate performance of the BiOCl@N-CNTs in this work are superior to most reported anode materials for Li/Na/K ion batteries.

| **Electrode** | **Current density (mA g$^{-1}$)** | **Cycle number** | **Capacity (mA h g$^{-1}$)** | **Batteries** | **Ref** |
|---|---|---|---|---|---|
| BiOBr@C | 100 | 100 | 422 | LIBs | [1] |
| BiOI nanosheets | 30 | initial | 717 | LIBs | [2] |
| BiOCl nanosheets | 50 | 15 | 254 | LIBs | [3] |
| BiOBr nanosheets | | | 230 | | |
| BiOCl ultrathin nanoplates | 10 | initial | 1050 | SIBs | [4] |
| BiOCl nanosheets | 50 | 100 | 70 | SIBs | [5] |

| | | | | | |
|---|---|---|---|---|---|
| Bilayer-$Bi_{12}O_{17}Cl_2$ nanosheets | 10 | 1500 | 198 | PIBs | [6] |
| Bismuth oxychloride nanoflake | 50 | 50 | 213 | PIBs | [7] |
| BiOCl/G | 50 | 50 | 251 | PIBs | [8] |
| **BiOCl@N-CNTs** | **100** | **100** | **315** | **PIBs** | **This work** |
| | **1000** | **2000** | **159** | | |

**Table S2.** The fitting values for the resistance of the electrodes in **Fig. S12**.

| Electrode | BiOCl@N-CNTs | | | | BiOCl@C |
|---|---|---|---|---|---|
| Cycle number | 0 | 1 | 20 | 50 | 0 |
| $R_S$ (Ω) | 7.343 | 4.949 | 4.945 | 5.186 | 6.003 |
| $R_{ct}$ (Ω) | 1007 | 1542 | 2350 | 2264 | 1738 |

**References**


1 X. Shi, H. Liu, J. Tian, P. Ning, J. Zhang and X. Shi, *Inorg. Chem. Commun.*, 2021, 125, 108415.

2 C. Chen, P. Hu, X. Hu, Y. Mei and Y. Huang, *Chem. Commun.*, 2015, 51, 2798-2801.

3 L. Ye, L. Wang, H. Xie, Y. Su, X. Jin and C. Zhang, *Energy Technology*, 2015, 3, 1115-1120.

4 Y. Zhang, S. Lu, M.-Q. Wang, Y. Niu, S. Liu, Y. Li, X. Wu, S.-J. Bao and M. Xu, *Mater. Lett.*, 2016, 178, 44-47.

5 P. K. Dutta, Y. Myung, R. Kulangaramadom Venkiteswaran, L. Mehdi, N. Browning, P. Banerjee and S. Mitra, *J. Phys. Chem. C*, 2019, 123, 11500-11507.

6 J. Zhu, J. Fan, T. Cheng, M. Cao, Z. Sun, R. Zhou, L. Huang, D. Wang, Y. Li and Y. Wu, *Nano Energy*, 2020, 75, 104939.

7 W. Li, Y. Xu, Y. Dong, Y. Wu, C. Zhang, M. Zhou, Q. Fu, M. Wu and Y. Lei, *Chem. Commun.*, 2019, 55, 6507-6510.

8 L. Ma, X. Li, Z. Li, Y. Zhang, Z. Ji, H. Wang, W. Mai, J. Li and L. Pan, *J. Colloid Interface Sci.*, 2021, 599, 857-862.